JPET Fast Forward. Published on April 5, 2016 as DOI: 10.1124/jpet.116.232215
This article has not been copyedited and formatted. The final version may differ from this version.

PROTECTION FROM CIGARETTE SMOKE-INDUCED LUNG DYSFUNCTION AND DAMAGE BY H2 RELAXIN (SERELAXIN)

Alessandro Pini, Giulia Boccalini, Laura Lucarini, Stefano Catarinicchia, Daniele Guasti, Emanuela Masini, Daniele Bani and Silvia Nistri

Department of Experimental & Clinical Medicine: Section of Anatomy & Histology & Research Unit of Histology & Embryology (AP, GB, SC, DG, DB, SN);

Department NEUROFARBA, Section of Pharmacology (LL, EM);

University of Florence. Florence, Italy

Running title: RELAXIN PREVENTS SMOKE-INDUCED LUNG INJURY

Corresponding author:

Dr. Silvia Nistri

Dept. Experimental & Clinical Medicine; Sect. Anatomy & Histology & Research Unit of Histology & Embryology. University of Florence. viale G.Pieraccini, 6. I-50139 Florence, Italy

Phone: +39 055 2758 156 silvia.nistri@unifi.it

Text pages 27

Figures 7

Tables 2

References 51

Words in the abstract 245

Words in the introduction 474

Words in the discussion 933

Nonstandard abbreviations

ELISA: enzyme-linked immuno-sorbent assay

CO: carbon monoxide

CS: cigarette smoke

COPD: chronic obstructive pulmonary disease

IL: interleukin

MPO: myeloperoxidase

OD: optical density

PAS: periodic acid-Schiff

RLX: serelaxin (recombinant human H2 relaxin)

ROI: region of interest

TNF: tumor necrosis factor

Section

Gastrointestinal, Hepatic, Pulmonary, and Renal

Abstract

Cigarette smoke (CS) is the major etiologic factor of chronic obstructive pulmonary disease (COPD), characterized by airway remodeling, lung inflammation and fibrosis, emphysema and respiratory failure. The current therapies can improve COPD management but cannot arrest its progression and reduce mortality. Hence, there is a major interest in identifying molecules susceptible of development into new drugs to prevent or reduce CS-induced lung injury. Serelaxin (RLX), or recombinant human relaxin-2, is a promising candidate because of its anti-inflammatory and antifibrotic properties highlighted in lung disease models. Here we used a guinea pig model of CS-induced lung inflammation and remodeling reproducing some of the hallmarks of COPD. Animals exposed chronically to CS (8 weeks) were treated with vehicle or RLX, delivered by osmotic pumps (1 or 10 μg/day) or aerosol (10 μg/ml/day) during CS treatment. Controls were non-smoking animals. RLX maintained airway compliance to a control-like pattern, likely because of its capability to counteract lung inflammation and bronchial remodeling. In fact, treatment of CS-exposed animals with RLX reduced the inflammatory recruitment of leukocytes, accompanied by a significant reduction of the release of pro-inflammatory cytokines (TNFα, IL-1β). Moreover, RLX was able to counteract the adverse bronchial remodeling and emphysema induced by CS exposure by reducing goblet cell hyperplasia, smooth muscle thickening and fibrosis. Of note, RLX delivered by aerosol has shown a comparable efficacy to systemic administration in reducing CS-induced lung dysfunction and damage. In conclusion, RLX emerges as a new molecule to counteract CS-induced inflammatory lung diseases.

JPET Fast Forward. Published on April 5, 2016 as DOI: 10.1124/jpet.116.232215
This article has not been copyedited and formatted. The final version may differ from this version.

Introduction

Cigarette smoke (CS) contains thousands of noxious substances in the gas and particulate phase including carcinogens and toxic agents which come in contact with bronchi and alveoli and cause several pulmonary diseases, ranging from inflammatory disorders to tumors. In particular, CS is considered the major etiologic factor of chronic obstructive pulmonary disease (COPD) (Tuder and Petrache, 2012), which affects 15-20% of smokers (Chung and Adcock, 2008). COPD is characterized by persistent, progressive and not fully reversible airflow limitation associated with an increased chronic inflammatory response, mast cell activation (Mortaz et al., 2011), mucus gland hyperplasia and hypersecretion accompanied by structural changes to the airways and lungs (Global Initiative for Chronic Obstructive Lung Disease, 2013). These structural changes typically include increase in smooth muscle mass of small and medium airways, emphysema and fibrosis (Chmiel et al., 2002) which lead to progressive deterioration of lung function (Paz and Shoenfeld, 2010). The noxious substances in CS induce lung epithelial tissue damage by a mechanism involving the generation of a highly inflammatory environment (Rahman and Adcock, 2006; Rahman and Kinnula, 2012). Several studies have reported that CS causes the production by inflammatory cells of elevated levels of cytokines, such as TNF-α, IL-1β, IL-6 and IL-8 (Glossop et al., 2006; Churg et al., 2009). These mediators, acting as chemoattractants, recruit further neutrophils, macrophages and dendritic cells which, in turn, exacerbate the inflammatory process and initiate fibrosis. The current therapies, primarily based on anti-inflammatory drugs, have improved the management of this disease but cannot prevent its progression towards lung fibrosis and substantially reduce mortality. Hence, there is a major interest in the identification of molecules susceptible of development into new drugs that can prevent or reduce inflammatory lung injury (Barnes, 2008). In this context, serelaxin (RLX), the recombinant molecule corresponding to the human hormone relaxin-2 (Hossain and Wade, 2014), emerges as a feasible candidate. RLX, best known for its effects on reproduction (Sherwood, 2004), also exhibits anti-inflammatory and antifibrotic properties

(Masini et al., 2004; Samuel et al., 2007; Bonacchi et al., 2009). In a setting of allergic airway disease, RLX has been shown to inhibit infiltration of pro-inflammatory cells into the lung and adverse airway remodelling (Bani et al., 1997; Royce et al., 2009; 2014), promote dilation of alveolar blood capillaries and reduce the thickness of the air–blood barrier (Bani et al., 1997). In an *in vivo* model of fibrosis, RLX treatment markedly decreased bleomycin-induced lung fibrosis and improved alveolar thickening (Unemori et al., 1996). Consistently, RLX-deficient mice have been shown to undergo an age-related progression of lung fibrosis which is reversed by treatment with exogenous RLX (Samuel et al., 2003). The aim of this study is to evaluate the potential protective action of RLX in an *in vivo* guinea pig model of lung inflammation and remodeling induced by chronic exposure to CS, reproducing some of the hallmarks of COPD.

Materials and methods

Reagents. RLX was kindly provided by the RRCA Relaxin Foundation (Florence, Italy). Kentucky Reference cigarettes 3R4F, each containing 11 mg of total particulate matter, 9.4 mg of tar, and 0.73 mg of nicotine, were obtained from the Kentucky Tobacco Research Council (Lexington, KY). Unless otherwise specified, the other reagents used for the experiments were from Sigma-Aldrich (Milan, Italy).

Exposure of guinea pigs to CS. Male Hartley albino guinea pigs weighing 300-350 g were used for the experiments (Harlan, Correzzana, Italy). Animal handling and use complied with the European Community guidelines for animal care (2010/63/EU) and were approved by the Committee for Animal Care and Experimental Use of the University of Florence. The animals were housed on a 12 h light/dark cycle at 22°C room temperature and had free access to food and water. The experiments

JPET Fast Forward. Published on April 5, 2016 as DOI: 10.1124/jpet.116.232215
This article has not been copyedited and formatted. The final version may differ from this version.

were designed to minimize pain and the number of animals used. Sacrifice was carried out by decapitation. The animals were divided into the following experimental groups (n=6/group)

Group 1: Control untreated animals

Group 2: Animals exposed daily to CS for 8 weeks;

Group 3: Animals exposed daily to CS for 8 weeks and treated with RLX given by continuous subcutaneous (s.c.) infusion using osmotic minipumps (Alzet, DURECT Corporation, Cupertino, CA). The pumps were implanted 1 day before starting the exposure to CS on the back upon anesthesia (i.p. injection of ketamine hydrochloride, 100 mg/kg b.w. and xylazine, 15 mg/kg b.w.) and filled to deliver a daily dose of 1 μg for the whole duration of CS exposure;

Group 4: Animals exposed to CS and treated with RLX given by minipumps as above, but delivering a daily RLX dose of 10 μg for the whole duration of CS exposure.

Group 5: Animals exposed to CS and treated with RLX (10 μg/ml) administered by aerosol (1 ml) for 10 min/day before CS exposure.

The animals were subjected to CS exposure in a smoke chamber, according to Das et al. (2012) with minor modifications. The smoke chamber (2.5 liters) was similar to a vacuum desiccator equipped with an open tube for cigarette positioning at one end and a vacuum-connected tube and stopcock at the opposite end. To each group of CS-exposed animals, five 3R4F reference cigarettes were administered daily. Each cigarette was fitted on the inlet tube and lit; then, a puff of CS was introduced into the chamber containing the animals by applying a mild suction of 4 cm water for 20 s. The guinea pigs were exposed to the accumulated smoke for further 40 s, for a total duration of CS exposure of 60 sec. After a pause of 60 s. during which the chamber was opened and ventilated with fresh air, a second puff was administered with the same procedure. The gap between each of the 5 cigarettes/day was 1 h. At the end of the treatment, the animals were anesthetized by i.p. injection of ketamine hydrochloride (100 mg/kg b.w.) and xylazine (15 mg/kg b.w.), blood and tissue samples were collected and processed for functional, morphological and biochemical analyses, as detailed below.

JPET Fast Forward. Published on April 5, 2016 as DOI: 10.1124/jpet.116.232215
This article has not been copyedited and formatted. The final version may differ from this version.

Functional study and tissue sampling. At the end of the treatment period, the animals were subjected to measurement of airway resistance to inflation, a functional parameter related to fibrosis-induced lung stiffness, by using a constant volume mechanical ventilation method (Masini et al., 2005). Briefly, upon anesthesia, the guinea pigs were operated on to insert a cannula into the trachea and then ventilated with a small-animal respirator (Ugo Basile, Comerio, Italy), adjusted to deliver a tidal volume of 9 ml at a rate of 40 strokes/min. Changes in lung resistance to inflation (pressure at the airway opening: PAO) were registered by a high-sensitivity pressure transducer (P75 type 379; Harvard Apparatus Inc. Holliston, MA) connected to a polygraph (Harvard Apparatus Inc.; settings: gain 1, chart speed 25 mm/s). Inflation pressure was measured for at least 3 min. In each animals, PAO measurements (expressed in mm on the chart) were carried out on at least 40 consecutive tracings of respiratory strokes and then averaged.

After PAO measurements, the animals were subjected to blood sampling by left ventricular puncture and killed by decapitation. After sacrifice, the chest was opened, the lungs were quickly excised and cut in fragments: some of them were processed for light and electron microscopy, others were weighed and homogenized in cold phosphate-buffered saline (PBS), 0.2 M, pH 6, supplemented with protease inhibitors (1mM PMSF, 20 μg/ml leupeptin, 1 μg/ml pepstatin, 1 mg/ml Pefabloc SC, 2.5 μg/ml aprotinin; Sigma) in a ratio of 100 μl/10 mg of tissue. The homogenates were centrifuged at 10,000 g for 30 min. at 4°C, the supernatants were collected and stored at -80°C until needed.

Detection of free carbon monoxide (CO) in plasma. Free CO was measured in the plasma of the animals of the different experimental groups as an index of the degree of exposure to CS. The amount of free CO in plasma was measured with an gaseous CO detector (RGA3, Reduction Gas Analyzer, SAES Getters, Milan, Italy) as described (Vreman et al., 1984). Measurements were

obtained by comparison with a CO standard curve prepared immediately before analysis and expressed as parts per million (ppm).

Determination of serum RLX levels. The circulating RLX levels were determined in guinea pig serum by ELISA (R&D Systems, Minneapolis, MN) according to the manufacturer's instructions.

Detection of lung myeloperoxidase (MPO). MPO is contained in the granules of neutrophils and monocytes/macrophages and is considered a reliable marker for leukocyte accumulation in the inflamed tissues (Mullane et al., 1985). MPO immunoreactivity was determined in paraformaldehyde-fixed, paraffin-embedded sections. Antigen retrieval was obtained in sodium citrate buffer (10 mM, pH 6.0, Bio-Optica). The sections were treated with 0.3% (v/v) H_2O_2 in PBS for 20 min to block endogenous peroxidase, incubated in 2 mg/ml glycine for 10 min and permeabilized with 0.1% (w/v) Triton X 100 in PBS for 20 minutes. Aspecific signal was quenched with 1% BSA in PBS for 20 min at room temperature. The sections were immunolabeled by incubation in: i) rabbit polyclonal anti-MPO (AbCam Cambrigde, UK) 1:50 in PBS, 4°C overnight; ii) biotinylated polyclonal goat anti-rabbit antiserum, 1:300 in PBS at room temperature, 2 h; iii) ABC Reagent (Vectastain ABC/Elite Kit, Vector Laboratories, Burlingame, CA, USA) for 20 min. Immune reaction was revealed using 3% H_2O_2 as substrate and 3-3' diaminobenzidine as chromogen. Finally, nuclei were counterstained with hematroxylin. Negative controls were carried out by omitting the primary antiserum.

MPO activity was also measured in the supernatant of lung tissue homogenates (100 μl), allowed to react with a solution of tetramethylbenzidine (1.6 mM) and 0.1 mM H_2O_2. The rate of change in absorbance was measured by a spectrophotometer (Perkin Elmer, Milan, Italy) at 650 nm. MPO activity was defined as the enzyme amount degrading 1 μmol of H_2O_2 /min at 37°C and was expressed in units/ml of supernatant.

JPET Fast Forward. Published on April 5, 2016 as DOI: 10.1124/jpet.116.232215
This article has not been copyedited and formatted. The final version may differ from this version.

Determination of serum and lung tissue cytokines. The levels of the pro-inflammatory cytokines TNF-α and IL-1 β and of the anti-inflammatory cytokine IL-10 were measured on guinea pig serum and supernatant of lung tissue homogenates using the FlowCytomix assay (Bender Medsystems GmbH, Vienna, Austria), according to the manufacturer′s instructions. Briefly, anti-cytokine Ig-coated beads were incubated with serum or supernatant samples and then with biotin-conjugated secondary antibodies and streptavidin-phycoerythrin. Fluorescence was read with a cytofluorimeter (CyFlow Space, Partec, Carate Brianza, Milan, Italy). Measurements were obtained by comparison with TNF-α, IL-1β or IL-10 standard curves and expressed as pg/ml.

Evaluation of lung tissue fibrosis. For assessment of lung collagen content, tissue sections from fragments fixed with 4% paraformaldehyde were stained with Picrosirius red in a single session to minimize artifactual differences in collagen staining. Optical density (OD) measurements of the deep red-stained collagen fibers were carried out by using the ImageJ 1.33 image analysis program (http://rsb.info.nih.gov/ij) upon selection of an appropriate threshold to include the stained tissue surface area. Values are reported as arbitrary units, calculated as surface area x OD x 10^{-6} (Pini et al., 2010) and represent the means ± SEM of the measurements of individual animals (at least twenty images each) from the different experimental groups.

Lung tissue fibrosis was also evaluated by hydroxyproline assay. Briefly, the frozen lung tissue was lyophilized for 48 hours and then thoroughly homogenized in distilled water. The samples were gently mixed with 12 M hydrochloric acid and hydrolyzed by autoclaving at 120 °C for 40 minutes in sealed polypropylene tubes, 2 ml volume. Chloromine T was added to the hydrolysate and allowed to react for 25 min at room temperature. Finally, Ehrlich's aldehyde reagent was added to the samples, incubated at 65°C for 20 min and the absorbance of the mixture was read spectrophotometrically at 550 nm.

Evaluation of lung tissue remodeling. Morphometry of smooth muscle layer thickness and bronchial goblet cell numbers, both key markers of airway remodeling, were performed on lung tissue sections stained with hematoxylin and eosin or with periodic acid-Schiff (PAS) staining for mucins, respectively. Digital photomicrographs of medium- and small-sized bronchi were randomly taken. Measurements of the thickness of the bronchial smooth muscle layer were carried out on the digitized images using the ImageJ 1.33 software. PAS-stained goblet cells and total bronchial epithelial cells were counted on bronchial cross-section profiles, and the percentage of goblet cells was calculated. For both parameters, values are means ± SEM of individual animals (twenty images each) from the different experimental groups.

The lung tissue sections stained with hematoxylin and eosin were also used to evaluate the cross-section surface area of alveolar air spaces, an index of lung emphysema. Determinations were performed on 3 randomly-chosen microscopical fields per animal viewed with a x10 objective. At the chosen magnification, each field corresponds to a tissue area of 90,200 μm^2 that includes about 50-100 air space profiles. Surface area measurements were carried out on digital micrographs using the ImageJ 1.33 image analysis software upon selection of an appropriate threshold to include only blank, tissue-free air spaces. Values are means ± SEM of alveolar lumenal areas calculated for each experimental group.

Transmission electron microscopy. Lung tissue samples taken at sacrifice were fixed in 4% glutaraldehyde and 1% osmium tetroxide and embedded in Epon 812. Ultrathin sections were stained with uranyl acetate and alkaline bismuth subnitrate and examined under a JEM 1010 electron microscope (Jeol,Tokyo, Japan) at 80 kV.

JPET Fast Forward. Published on April 5, 2016 as DOI: 10.1124/jpet.116.232215
This article has not been copyedited and formatted. The final version may differ from this version.

Results

Evaluation of CS exposure. To check the effectiveness of the animal model, the levels of plasma free carbon monoxide (CO) were measured as an index of exposure to CS. Compared with the controls, the animals of the different experimental groups chronically exposed to CS had significantly elevated CO levels. No differences were detected among the CS-exposed groups, suggesting that all the animals were subjected to the same degree of CS-induced toxicity (Table 1)

Plasma RLX levels. The circulating levels of RLX evaluated at the end of the experiment were 30±4.4 pg/ml and 1.1±0.1 ng/ml upon 1 and 10 μg daily doses, respectively. The values measured in the aerosol-treated animals were consistently below the detection threshold, as were those of the untreated controls and the CS-exposed animals not given RLX.

Evaluation of respiratory dysfunction. CS exposure caused a statistically significant decrease in airway compliance, as judged by the clear-cut elevation of pressure at the airway opening (PAO), compared with the controls. Administration of RLX by osmotic pumps at both doses and by aerosol induced a statistically significant increase in airway compliance in respect with the CS-exposed animals (Figure 1).

Evaluation of airway inflammation. CS exposure induced substantial airway inflammation. In fact, compared with the controls, CS caused a significant increase in MPO-immunoreactive leukocytes infiltrating the lungs, which was significantly reduced by administration of RLX by osmotic pumps at both doses and by aerosol (Figure 2 A). Accordingly, CS caused a marked elevation of lung MPO activity as compared with the controls, which was significantly antagonized by RLX given systemically at both doses or by aerosol (Figure 2 B).

JPET Fast Forward. Published on April 5, 2016 as DOI: 10.1124/jpet.116.232215
This article has not been copyedited and formatted. The final version may differ from this version.

CS also induced a significant increase in serum and lung tissue levels of the pro-inflammatory cytokines TNF-α and IL-1β and decrease in the levels of anti-inflammatory IL-10. These effects of CS were reduced by RLX administered systemically or by aerosol (Figure 3 A-C).

Evaluation of airway remodeling and emphysema. Picrosirius-red staining and morphometry, performed to evaluate lung fibrosis, showed a sharp, statistically significant increase in collagen fibers in the peri-bronchiolar regions of the CS-exposed guinea pigs compared with the controls, while administration of RLX by osmotic pumps at both doses and by aerosol resulted in a significant inhibition of CS-induced fibrosis (Figure 4 A). Accordingly, CS exposure caused a significant increase in lung tissue hydroxyproline content, an index of collagen amount, as compared with the controls, whereas RLX with every delivery protocol markedly reduced it (Figure 4 B).

RLX also reduced the histological changes induced by CS in the bronchiolar wall which are considered as markers of remodeling. Namely, the percentage of PAS-positive goblet cells over total bronchial epithelial cells (Figure 5), as well as the thickness of the airway smooth muscle layer (Figure 6), were significantly increased in the CS-exposed guinea pigs compared with the controls, while administration of RLX by osmotic pumps at both doses and by aerosol significantly reduced these parameters of airway remodeling (Figures 5,6). Morphometry of the mean cross-section area (±SEM) of the distal alveolar air spaces (Table 2) showed that these appeared enlarged in the CS-exposed guinea pigs compared with the controls, indicating the occurrence of emphysema. This feature was reduced upon treatment with RLX at any doses and administration pathways. Due to broad SEM variations and the limited number of guinea pigs per group, these differences did not reach statistical significance.

Lung remodeling was also investigated by transmission electron microscopy (Figure 7). The control lungs showed normal features of the bronchiolar and alveolar parenchyma and the surrounding stromal components. In particular, bronchioles were mostly lined by ciliated cells and a

JPET Fast Forward. Published on April 5, 2016 as DOI: 10.1124/jpet.116.232215
This article has not been copyedited and formatted. The final version may differ from this version.

minority of bronchiolar (or Clara) cells with exocrine features; the epithelial lining was surrounded by a loose lamina propria including bundles of smooth muscle cells. CS caused prominent ultrastructural abnormalities, mainly consisting in reduced size of surface epithelial cells, some of which showed signs of demise, and marked fibrosis of the lamina propria causing disruption of the architecture of the smooth muscle layers; inflammatory cells were often found. Administration of RLX by osmotic pumps at both doses and by aerosol markedly reduced the CS-induced abnormalities of lung bronchioles. In all the CS-exposed experimental groups, the most distal, alveolar/capillary lung components did not show substantial changes as compared with the controls (data not shown).

Discussion

In the present study we have exploited a guinea pig model of chronic lung inflammation and remodeling to provide evidence that RLX protects against lung dysfunction and damage induced by chronic exposure to CS. In this model, which reproduces some of the hallmarks of COPD of smokers, the administration of RLX to guinea pigs along with chronic CS exposure prevents the occurrence of lung damage and maintains airway compliance to a control-like pattern. This action of RLX is likely due to its capability to counteract lung inflammation and bronchial remodeling. In fact, treatment of CS-exposed guinea pigs with RLX reduces the inflammatory recruitment of leukocytes, as judged by the observed decrease in MPO-immunoreactive cells and in lung MPO activity in respect with the CS-exposed animals not given RLX. In keeping with these findings, RLX caused a significant reduction of the release of the pro-inflammatory cytokines TNFα and IL-1β while it maintained nearly normal levels of the anti-inflammatory cytokine IL-10. Moreover, RLX was able to counteract the adverse bronchial remodeling induced by CS exposure by reducing goblet cell hyperplasia, smooth muscle wall thickening and fibrosis, and to blunt emphysema of the distal air spaces. These effects of RLX fit well with previous reports that this hormone reduces

JPET Fast Forward. Published on April 5, 2016 as DOI: 10.1124/jpet.116.232215
This article has not been copyedited and formatted. The final version may differ from this version.

inflammation and fibrosis in many *in vitro* and *in vivo* models of disease (Masini et al., 1994;2004; Nistri et al., 2003;2008; Lekgabe et al., 2005; Bonacchi et al., 2009; Sasser, 2013; Royce et al., 2014; Samuel et al., 2014). In particular, RLX and RLX receptor agonists have been shown to prevent the development of airway sclerosis and remodeling in a bleomycin-induced model of lung fibrosis (Unemori et al., 1996; Pini et al., 2010), as well as in rodent models of allergic asthma-like reaction (Bani et al., 1997; Kenyon et al., 2003).

A limitation of the present study, which was primarily designed to investigate whether RLX could interfere with the pathogenic events of CS-induced pulmonary injury, consists in lack of the direct demonstration that RLX may be beneficial on established lung damage. Further studies are thus required to explore the actual therapeutic potential of RLX, considering that when smokers come into the clinic with COPD, the initial damage has been done, the disease progresses from there, and the appropriate therapy should be able to revert it to health. Nonetheless, the present findings and others from the literature bolster the hypothesis that RLX deserves to be further investigated as a new drug for the treatment of CS-induced COPD. Indeed, the current therapies for COPD, primarily based on corticosteroids and bronchodilators, have improved disease management but cannot prevent disease progression (Barnes, 2010; Kabir and Morshed, 2015). Rather, at the doses and administration times effective to control COPD, glucocorticoids can cause unwanted local and systemic side effects (Kelly and Nelson, 2003). Even the most recent cell therapy trials, based on the principle that grafted bone marrow-derived mesenchymal stem cells can exert immunomodulatory and anti-inflammatory effects (Aggarwal and Pittenger, 2005; Krampera et al., 2006; Gupta et al., 2007; Song et al., 2012), did not meet the expectations because they failed to induce major, durable improvements in lung function or quality of life (Weiss et al., 2013). Therefore, the possibility that RLX could be developed as a new therapeutic tool for the management of COPD, alone or in combination with corticosteroids or other drugs and/or cell therapy, is relevant to human health. In this context, a recent study with an experimental model of allergic airway disease has shown that combination therapy with RLX and methylprednisolone

JPET Fast Forward. Published on April 5, 2016 as DOI: 10.1124/jpet.116.232215
This article has not been copyedited and formatted. The final version may differ from this version.

augments the effects of either treatment alone in inhibiting subepithelial fibrosis (Royce et al., 2013). Along this line of thought, RLX was shown to improve the grafting and anti-fibrotic efficacy of stem cell therapy for organ repair in various in vivo models (Formigli et al., 2007; Bonacchi et al., 2009; huuskes et al., 2015). The possibility that RLX may be therapeutically effective in COPD is further supported by the results of an experimental *in vivo* study on ageing-related vascular damage which have shown that RLX treatment possesses the unique ability to not only prevent but also revert established arterial remodeling and fibrosis (Xu et al., 2010).

In the present study, RLX delivered by aerosol has shown a comparable efficacy to systemic administration in reverting CS-induced lung dysfunction and damage, suggesting that this route of administration of RLX is therapeutically effective, at least in the lung. Moreover, the finding of undetectable levels of RLX in the plasma of the aerosol-treated animals accounts for a local action of this hormone on lung tissues. This possibility is supported by the observation that the specific RLX receptor RXFP1 is expressed by lung tissues (Samuel et al., 2003; Scott et al., 2004; Royce et al., 2014). The aerosol route of delivery is particularly attractive because it offers easier use and better patients' compliance than systemic delivery. In recent years, there has been intensive development of inhaled protein therapeutics for several disease conditions, such as inhaled insulin for the treatment of diabetes or inhaled interferon-γ for idiopathic pulmonary fibrosis (Hickey, 2013). In this context, a recent study (Royce et al., 2014) has shown that intranasally administered RLX abrogates airway hyperresponsiveness and remodeling in a mouse model of allergic asthma-like disease.

The hypothesis that RLX may be developed as a new drug for the treatment of COPD, alone or in combination with other therapeutics, is strengthened by the favorable outcome of a recent clinical trial in heart failure patients (Teerlink et al., 2013), which also revealed that RLX administration is safe and free of adverse side effects (Bani et al., 2009; Bani and Bigazzi, 2011).

Acknowledgments

We gratefully acknowledge the RRCA Relaxin Foundation (Florence, Italy) for the generous gift of serelaxin (RLX).

Authorship contributions

Participated in research design: Pini, Bani, Nistri.

Conducted experiments: Pini, Boccalini, Lucarini, Catarinicchia, Guasti, Masini, Bani, Nistri

Performed data analysis: Boccalini, Masini, Bani,

Wrote or contributed to the writing of the manuscript: Pini, Bani, Nistri

References

Aggarwal S, Pittenger MF (2005) Human mesenchymal stem cells modulate allogeneic immune cell responses. *Blood* **105**: 1815–1822.

Bani D, Ballati L, Masini E, Bigazzi M, Bani Sacchi T (1997) Relaxin counteracts asthma-like reaction induced by inhaled antigen in sensitized guinea pigs. *Endocrinology* **138**: 1909-1915.

Bani D, Bigazzi M (2011) Relaxin as a cardiovascular drug: a promise kept. *Curr Drug Saf* **6**: 324-328.

Bani D, Yue SK, Bigazzi M (2009) Clinical profile of relaxin, a possible new drug for human use. *Curr Drug Saf* **4**: 238-249.

Barnes PJ (2008) Emerging pharmacotherapies for COPD. *Chest* **134**: 1278-1286.

Barnes PJ (2010) Inhaled corticosteroids in COPD: a controversy. *Respiration* **80**: 89-95.

Bonacchi M, Nistri S, Nanni C, Gelsomino S, Pini A, Cinci L, Maiani M, Zecchi-Orlandini S, Lorusso R, Fanti S, Silvertown J, Bani D (2009) Functional and histopathological improvement of the post-infarcted rat heart upon myoblast cell grafting and relaxin therapy. *J Cell Mol Med* **13**: 3437-3448.

Chmiel JF, Berger M, Konstan MW (2002) The role of inflammation in the pathophysiology of CF lung disease. *Clin. Rev Allergy Immunol* **23**: 5–27.

Chung KF, Adcock IM (2008) Multifaceted mechanisms in COPD: inflammation, immunity, and tissue repair and destruction. *Eur Respir J* **31**: 1334-1356.

Churg A, Zhou S, Wang X, Wang R, Wrigh, JL (2009) The role of interleukin-1beta in murine cigarette smoke-induced emphysema and small airway remodeling. *Am J Respir Cell Mol Biol* **40**: 482–490.

Das A, Dey N, Ghosh A, Das S, Chattopadhyay DJ, Chatterjee IB (2012) Molecular and cellular mechanisms of cigarette smoke-induced myocardial injury: prevention by vitamin C. PLoS One doi: 10.1371/journal.pone.0044151.

Formigli L, Perna AM, Meacci E, Cinci L, Margheri M, Nistri S, Tani A, Silvertown J, Orlandini G, Porciani C, Zecchi-Orlandini S, Medin J, Bani D (2007) Paracrine effects of transplanted myoblasts and relaxin on post-infarction heart remodelling. *J Cell Mol Med* **11**: 1087-1100.

Global Initiative for Chronic Obstructive Lung Disease (GOLD). (2013) Global Strategy for Diagnosis Management and Prevention of COPD. Available: http://goldcopd.org

Glossop JR, Dawes PT, Mattey DL (2006) Association between cigarette smoking and release of tumor necrosis factor alpha and its soluble receptors by peripheral blood mononuclear cells in patients with rheumatoid arthritis. *Rheumatology (Oxford)* **45**: 1223–1229.

Gupta N, Su X, Popov B, Lee JW, Serikov V, Matthay MA (2007) Intrapulmonary delivery of bone marrow-derived mesenchymal stem cells improves survival and attenuates endotoxin-induced acute lung injury in mice. *J Immunol* **179**: 1855–1863.

Hickey AJ (2013) Back to the future: inhaled drug products. *J Pharm Sci* **102**: 1165–1172.

Hossain MA, Wade JD (2014) Synthetic relaxins. *Curr Opin Chem Biol* **22**: 47-55.

Huuskes BM, Wise AF, Cox AJ, Lim EX, Payne NL, Kelly DJ, Samuel CS, Ricardo SD (2015) Combination therapy of mesenchymal stem cells and serelaxin effectively attenuates renal fibrosis in obstructive nephropathy. *FASEB J* **29**: 540-553.

Kabir ER, Morshed N (2015) Different approaches in the treatment of obstructive pulmonary diseases. *Eur J Pharmacol* **764**: 306-317.

Kelly HW, Nelson HS (2003) Potential adverse effects of the inhaled corticosteroids *J Allergy Clin Immunol* **112**: 469-478.

Kenyon NJ, Ward RW, Last JA (2003) Airway fibrosis in a mouse model of airway inflammation. *Toxicol Appl Pharmacol* **186**: 90-100.

Krampera M, Pasini A, Pizzolo G, Cosmi L, Romagnani S, Annunziato F (2006) Regenerative and immunomodulatory potential of mesenchymal stem cells. *Curr Opin Pharmacol* **6**: 435–441.

Lekgabe ED, Kiriazis H, Zhao C, Xu Q, Moore XL, Su Y, Bathgate RA, Du XJ, Samuel CS (2005) Relaxin reverses cardiac and renal fibrosis in spontaneously hypertensive rats. *Hypertension* **46**: 412-418.

Masini E, Bani D, Bigazzi M, Mannaioni PF, Bani-Sacchi T (1994) Effects of relaxin on mast cells. In vitro and in vivo studies in rats and guinea pigs. *J Clin Invest* **94**: 1974–1980.

Masini E, Nistri S, Vannacci A, Bani Sacchi T, Novelli A, Bani D (2004) Relaxin inhibits the activation of human neutrophils: involvement of the nitric oxide pathway. *Endocrinology* **145**: 1106-1112.

Masini E, Bani D, Vannacci A, Pierpaoli S, Mannaioni PF, Comhair SA, Xu W, Muscoli C, Erzurum SC, Salvemini D (2005) Reduction of antigen-induced respiratory abnormalities and airway inflammation in sensitized guinea pigs by a superoxide dismutase mimetic. *Free Radic Biol Med* **39**: 520-531.

Mortaz E, Folkerts G, Redegeld F (2011) Mast cells and COPD. *Pulm Pharmacol Ther* **24**: 367-372.

Mullane KM, Kraemer R, Smith B (1985) Myeloperoxidase activity as a quantitative assessment of neutrophil infiltration into ischemic myocardium. *J Pharmacol Methods* **14**: 157-167.

Nistri S, Chiappini L, Sassoli C, Bani D (2003) Relaxin inhibits lipopolysaccharide-induced adhesion of neutrophils to coronary endothelial cells by a nitric oxide-mediated mechanism. *FASEB J* **17**: 2109-2111.

Nistri S, Cinci L, Perna AV, Masini E, Matroianni R, Bani D (2008) Relaxin induces mast cell inhibition and reduces ventricular arrhythmias in a swine model of acute myocardial infarction. *Pharmacol Res* **57**: 43-48.

Paz Z, Shoenfeld Y (2010) Antifibrosis: to reverse the irreversible. *Clin Rev Allergy Immunol* **38**: 276-286.

Pini A, Shemesh R, Samuel CS, Bathgate RA, Zauberman A, Hermesh C, Wool A, Bani D, Rotman G (2010) Prevention of bleomycin-induced pulmonary fibrosis by a novel antifibrotic peptide with relaxin-like activity. *J Pharmacol Exp Ther* **335**: 589-599.

Rahman I, Adcock IM (2006) Oxidative stress and redox regulation of lung inflammation in COPD. *Eur Respir J* **28**: 219-242.

Rahman I, Kinnula VL (2012) Strategies to decrease ongoing oxidant burden in chronic obstructive pulmonary disease. *Expert Rev Clin Pharmacol* **5**: 293-309.

Royce SG, Miao YR, Lee M, Samuel CS, Tregear GW, Tang ML (2009) Relaxin reverses airway remodeling and airway dysfunction in allergic airways disease. *Endocrinology* **150**: 2692-2699.

Royce SG, Sedjahtera A, Samuel CS, Tang ML (2013) Combination therapy with relaxin and methylprednisolone augments the effects of either treatment alone in inhibiting subepithelial fibrosis in an experimental model of allergic airways disease. *Clin Sci (Lond)* **124**: 41-51.

Royce SG, Lim CX, Patel KP, Wang B, Samuel CS, Tang ML (2014) Intranasally administered serelaxin abrogates airway remodelling and attenuates airway hyperresponsiveness in allergic airways disease. *Clin Exp Allergy* **44**: 1399-1408.

Samuel CS, Zhao C, Bathgate RA, Bond CP, Burton MD, Parry LJ, Summers RJ, Tang ML, Amento EP, Tregear GW (2003) Relaxin deficiency in mice is associated with an age-related progression of pulmonary fibrosis *FASEB J* **17**: 121-123.

Samuel CS, Hewitson TD, Unemori EN, Tang ML (2007) Drugs of the future: the hormone relaxin. *Cell Mol Life Sci* **64**: 1539-1557.

Samuel CS, Bodaragama H, Chew JY, Widdop RE, Royce SG, Hewitson TD (2014) Serelaxin is a more efficacious antifibrotic than enalapril in an experimental model of heart disease. *Hypertension* **64**: 315-322.

Sasser JM (2013) The emerging role of relaxin as a novel therapeutic pathway in the treatment of chronic kidney disease. *Am J Physiol Regul Integr Comp Physiol* **305**: R559-R565.

Scott DJ, Layfield S, Riesewijk A, Morita H, Tregear G, Bathgate RA (2004) Identification and characterization of the mouse and rat relaxin receptors as the novel orthologues of human leucine-rich repeat-containing g-protein-coupled receptor 7. *Clin Exp Pharmacol Physiol* **31**: 828-832.

Sherwood OD (2004) Relaxin's physiological roles and other diverse actions. *Endocr Rev* **25**: 205-234.

Song L, Xu JF, Qu JM, Sai Y, Chen CM, Yu L, Li D, Guo X (2012) A therapeutic role for mesenchymal stem cells in acute lung injury independent of hypoxia-induced mitogenic factor. *J Cell Mol Med* **16**: 376-385.

Teerlink JR, Cotter G, Davison BA, Felker GM, Filippatos G, Greenberg BH, Ponikowski P, Unemori E, Voors AA, Adams KF Jr, Dorobantu MI, Grinfeld LR, Jondeau G, Marmor A, Masip J, Pang PS, Werdan K, Teichman SL, Trapani A, Bush CA, Saini R, Schumacher C, Severin TM, Metra M; RELAXin in Acute Heart Failure (RELAX-AHF) Investigators (2013) Serelaxin, recombinant human relaxin-2, for treatment of acute heart failure (RELAX-AHF): a randomised, placebo-controlled trial. *The Lancet* **381**: 29-39.

Tuder RM, Petrache I (2012) Pathogenesis of chronic obstructive pulmonary disease. *J Clin Invest* **122**: 2749-2755.

Unemori EN, Pickford LB, Salles AL, Piercy CE, Grove BH, Erikson ME, Amento EP (1996) Relaxin induces an extracellular matrix-degrading phenotype in human lung fibroblasts in vitro and inhibits lung fibrosis in a murine model in vivo. *J Clin Invest* **98**: 2739-2745.

Vreman HJ, Kwong LK, Stevenson DK (1984) Carbon monoxide in blood: an improved microliter blood-sample collection system with rapid analysis by gas chromatography. *Clin Chem* **30**: 1382-1386.

Watanabe K, Jinnouchi K, Yagi T. (2002) Immunoreactivity for myeloperoxidase (MPO) in the vestibule after the injection of bacterial lipopolysaccharide into the middle ear. *Auris Nasus Larynx* **29**:241-245.

Weiss DJ, Casaburi R, Flannery R, LeRoux-Williams M, Tashkin DP (2013) A placebo-controlled, randomized trial of mesenchymal stem cells in COPD. *Chest* **143**: 1590-1598.

Xu Q, Chakravorty A, Bathgate RA, Dart AM, Du XJ (2010) Relaxin therapy reverses large artery remodeling and improves arterial compliance in senescent spontaneously hypertensive rats. *Hypertension* **5**: 1260-1266.

Footnote to the title

This work was supported by institutional funds from the University of Florence issued to Pini, Bani and Nistri

JPET Fast Forward. Published on April 5, 2016 as DOI: 10.1124/jpet.116.232215
This article has not been copyedited and formatted. The final version may differ from this version.

Figure legends

Figure 1 – Pressure at the airway opening (PAO), an index of respiratory dysfunction related to adverse airway remodeling. PAO is significantly increased by CS exposure as compared with the controls and reduced by administration of RLX by osmotic pumps at both doses and by aerosol. Values are means ± SEM (one-way ANOVA test), n=6. ### $p<0.001$ vs. controls; *** $p<0.001$ vs. CS-exposed animals.

Figure 2 – A) Lung MPO-immunoreactive leukocytes; B) lung tissue MPO activity. The number of MPO+ leukocytes and overall MPO activity are significantly increased by CS exposure as compared with the controls and reduced by administration of RLX by osmotic pumps at both doses and by aerosol. Values are means ± SEM (one-way ANOVA test), n=6. ### $p<0.001$ vs. controls; *** $p<0.001$, ** $p<0.01$ vs. CS-exposed animals. Magnification x400. Bar = 50 μm

Figure 3 – Levels of circulating (open bars) and lung tissue (striped bars) cytokines modulating inflammation. CS exposure causes an increase in pro-inflammatory TNF-α and IL-1β and decrease in anti-inflammatory IL-10 as compared with the controls. These effects were blunted by administration of RLX by osmotic pumps at both doses and by aerosol. Values are means ± SEM (one-way ANOVA test), n=6. ### $p<0.001$, ## $p<0.01$ vs. controls; * $p<0.05$, ** $p<0.01$, *** $p<0.001$ vs. CS-exposed animals.

Figure 4 – Airway fibrosis. The optical density of picrosirius red-stained collagen (A), and the levels of lung hydroxyproline (B), a marker of collagen amount, are significantly increased by CS exposure as compared with the controls and reduced by administration of RLX by osmotic pumps at both doses and by aerosol. Values are means ± SEM (one-way ANOVA test), n=6. ###

p<0.001, ## *p*<0.01 vs. controls; *** *p*<0.001, * *p*<0.05 vs. CS-exposed animals. Magnification x400. Bar = 50 μm

Figure 5 – Airway remodeling. The number of PAS+ goblet cells in the lining epithelium of small- and medium-sized bronchi are significantly increased by CS exposure as compared with the controls and reduced by administration of RLX by osmotic pumps at both doses and by aerosol. Values are means ± SEM (one-way ANOVA test), n=6. ### *p*<0.001 vs. controls; *** *p*<0.001, ** *p*<0.01, vs. CS-exposed animals. Magnification x400. Bar = 50 μm

Figure 6 – Airway remodeling. The thickness of the smooth muscle coat of small- and medium-sized bronchi is significantly increased by CS exposure as compared with the controls and reduced by administration of RLX by osmotic pumps at both doses and by aerosol. Values are means ± SEM (one-way ANOVA test), n=6. ### *p*<0.001 vs. controls; *** *p*<0.001, ** *p*<0.01, vs. CS-exposed animals. Magnification x400. Bar = 50 μm

Figure 7 - Representative electron micrographs of small-sized bronchi. In the untreated controls, bronchi are lined by ciliated cells and bronchiolar or Clara cells (C) containing secretion granules. In the CS-exposed animals, prominent abnormalities appear, consisting in reduced size and vaculation of surface epithelial cells and marked fibrosis of the lamina propria, with thick bundles of collagen fibers (asterisks) disrupting the architecture of the smooth muscle (SM) layers. Administration of RLX by osmotic pumps at the noted dose reduced the CS-induced abnormalities. Magnification x5000. Bar = 1 μm

JPET Fast Forward. Published on April 5, 2016 as DOI: 10.1124/jpet.116.232215
This article has not been copyedited and formatted. The final version may differ from this version.

Table 1 – Plasma free carbon monoxide levels

controls	**CS**	**CS+RLX 1 µg/day**	**CS+RLX 10 µg/day**	**CS+RLX aerosol**
6,4±0,8***	37,9±3,2	32,1±3,1	37,5±5,8	36,1±4,7

Values are mean ± SEM, n=6. Significance of differences (one-way ANOVA) ***p<0.001 vs. the other groups.

JPET Fast Forward. Published on April 5, 2016 as DOI: 10.1124/jpet.116.232215
This article has not been copyedited and formatted. The final version may differ from this version.

Table 2 – Mean cross-section area (µm^2) of alveolar air spaces.

controls	CS	CS+RLX 1 µg/day	CS+RLX 10 µg/day	CS+RLX aerosol
9759 ± 1203	13026 ± 634	10396 ± 332	11093 ± 1304	9644 ± 1528

Values are mean ± SEM, n=6. The differences do not reach statistical significance (one-way ANOVA)

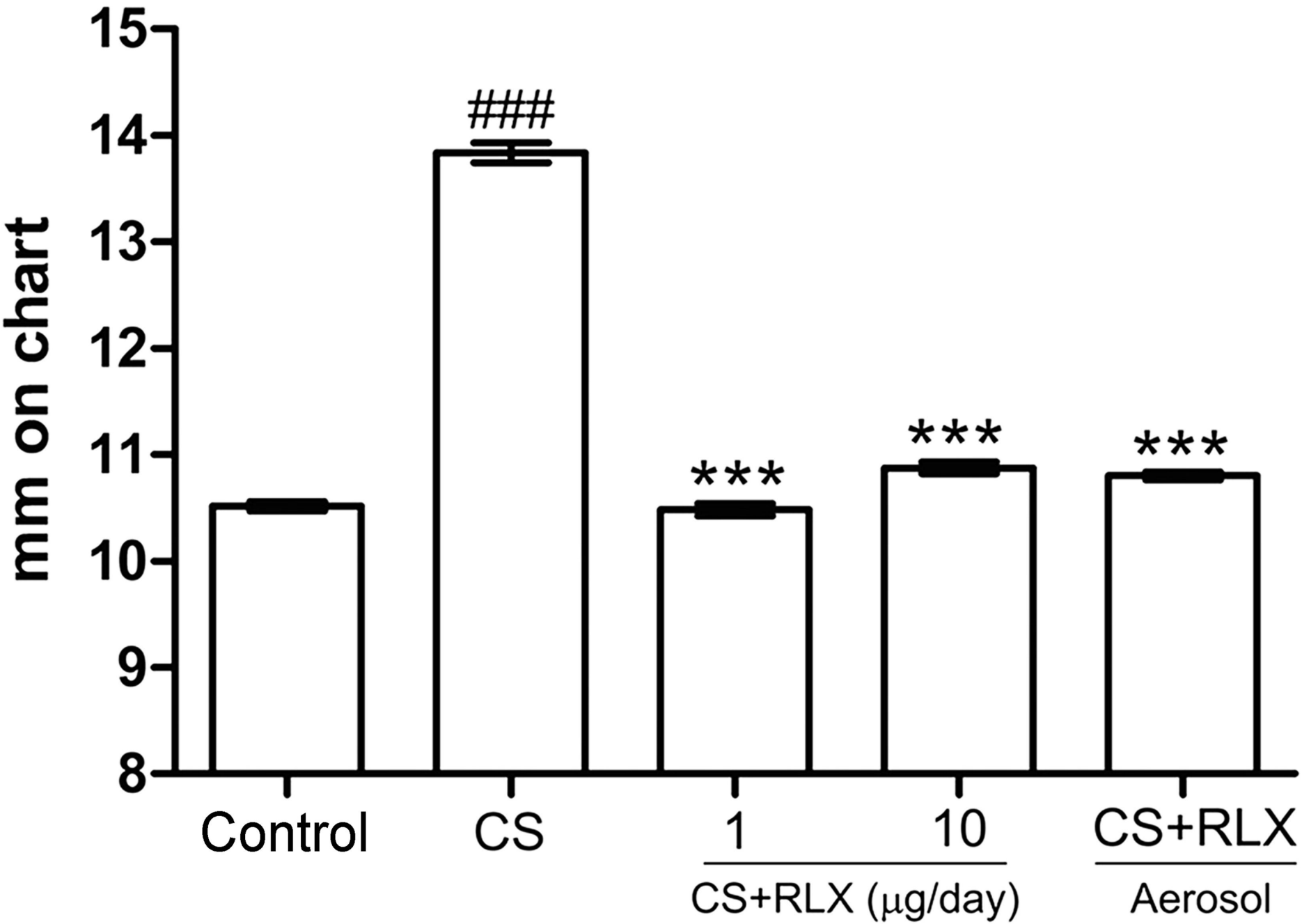
15
14
13
12
11
10
9
8
mm on chart
###
***
***
***
Control
CS
1
10
CS+RLX
CS+RLX (µg/day)
Aerosol

Figure 1

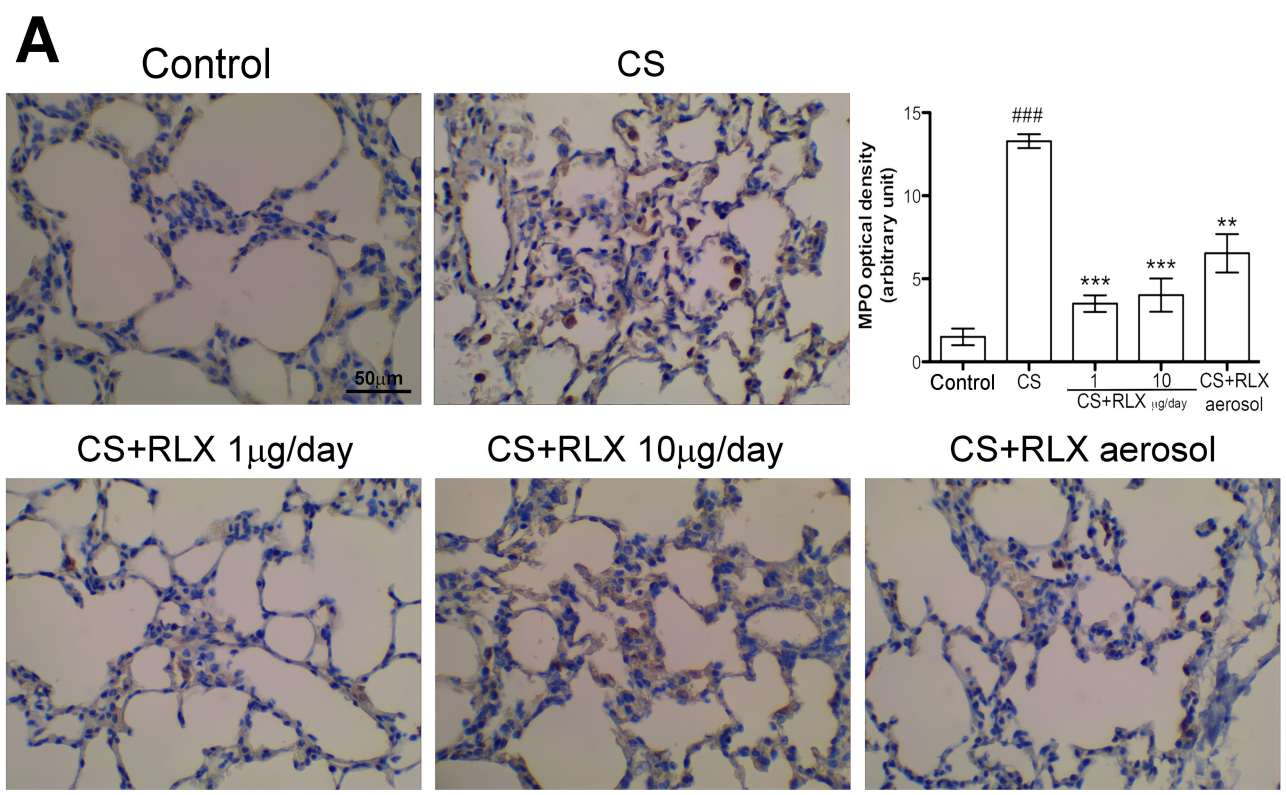
A
Control
CS
50μm
MPO optical density (arbitrary unit)
15
10
5
0
###
***
***
**
Control
CS
1
10
CS+RLX μg/day
CS+RLX aerosol
CS+RLX 1μg/day
CS+RLX 10μg/day
CS+RLX aerosol

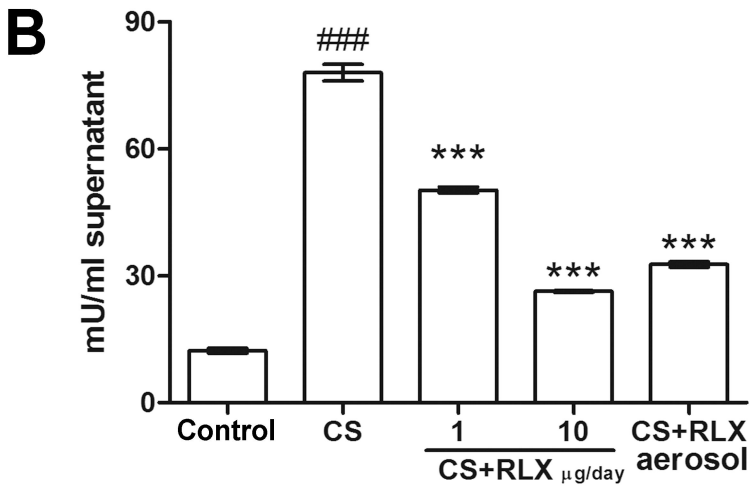
B
mU/ml supernatant
90
60
30
0
###
***
***
***
Control
CS
1
10
CS+RLX μg/day
CS+RLX aerosol

Figure 2

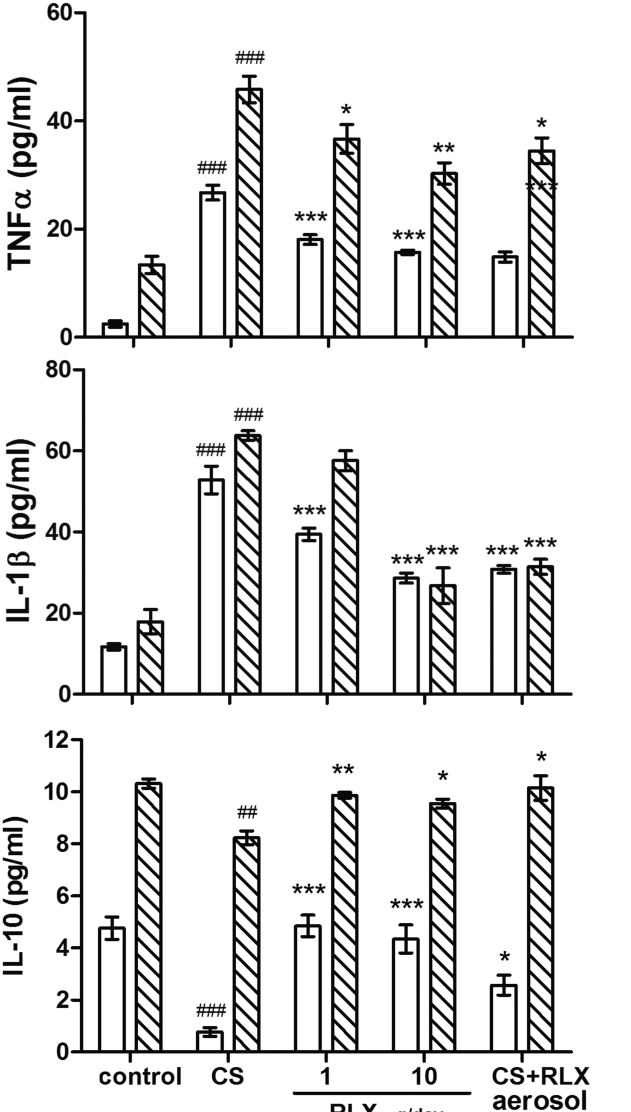
TNFα (pg/ml)
IL-1β (pg/ml)
IL-10 (pg/ml)
control
CS
1
10
CS+RLX aerosol
RLX μg/day

Figure 3

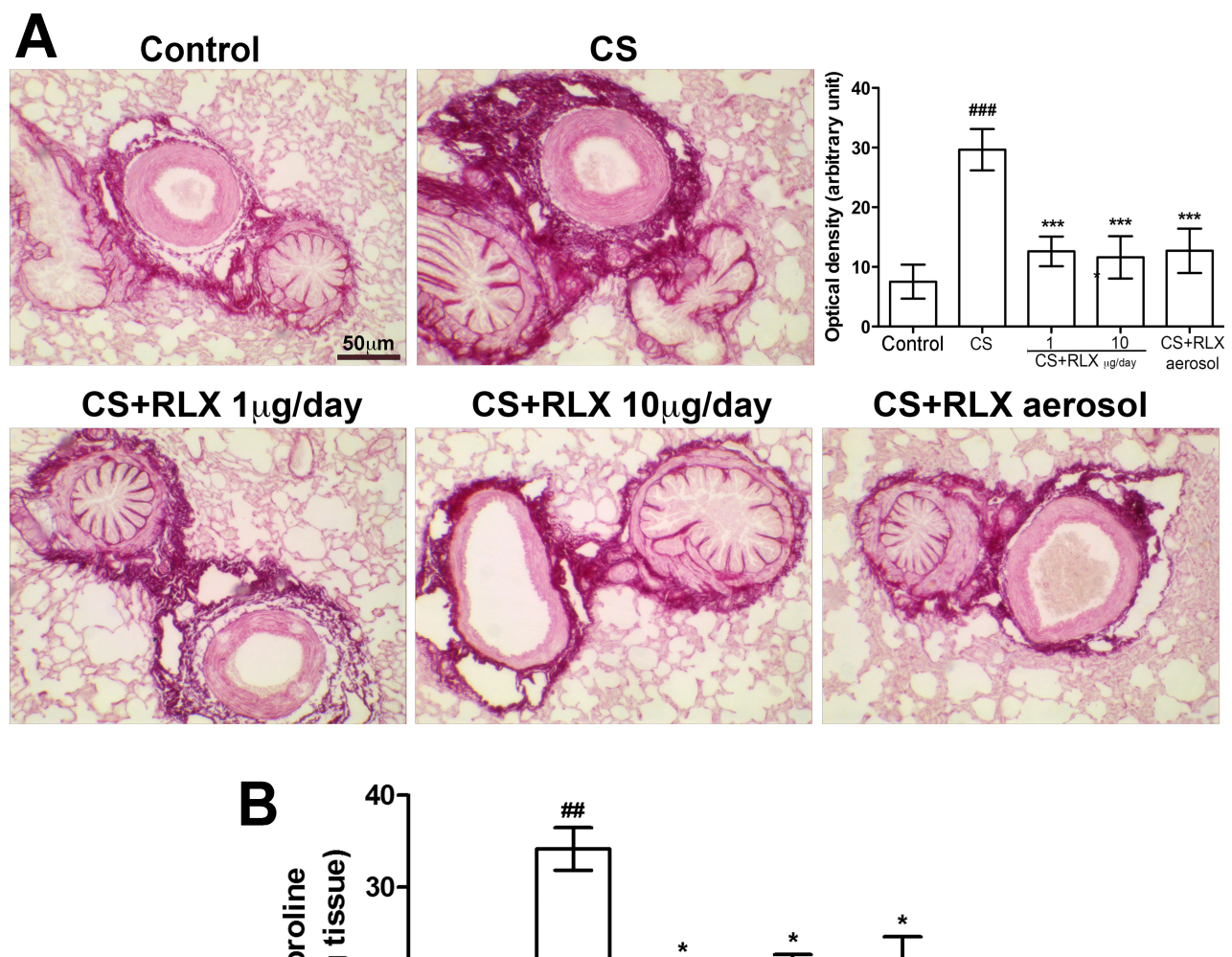
A
Control
CS
50μm
Optical density (arbitrary unit)
40
30
20
10
0
###
***
***
***
Control
CS
1
10
CS+RLX μg/day
CS+RLX aerosol
CS+RLX 1μg/day
CS+RLX 10μg/day
CS+RLX aerosol

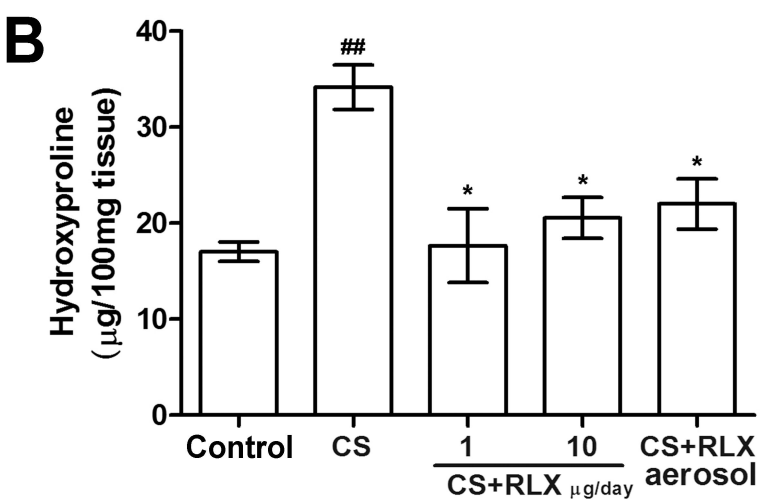
B
Hydroxyproline (μg/100mg tissue)
40
30
20
10
0
##
*
*
*
Control
CS
1
10
CS+RLX μg/day
CS+RLX aerosol

Figure 4

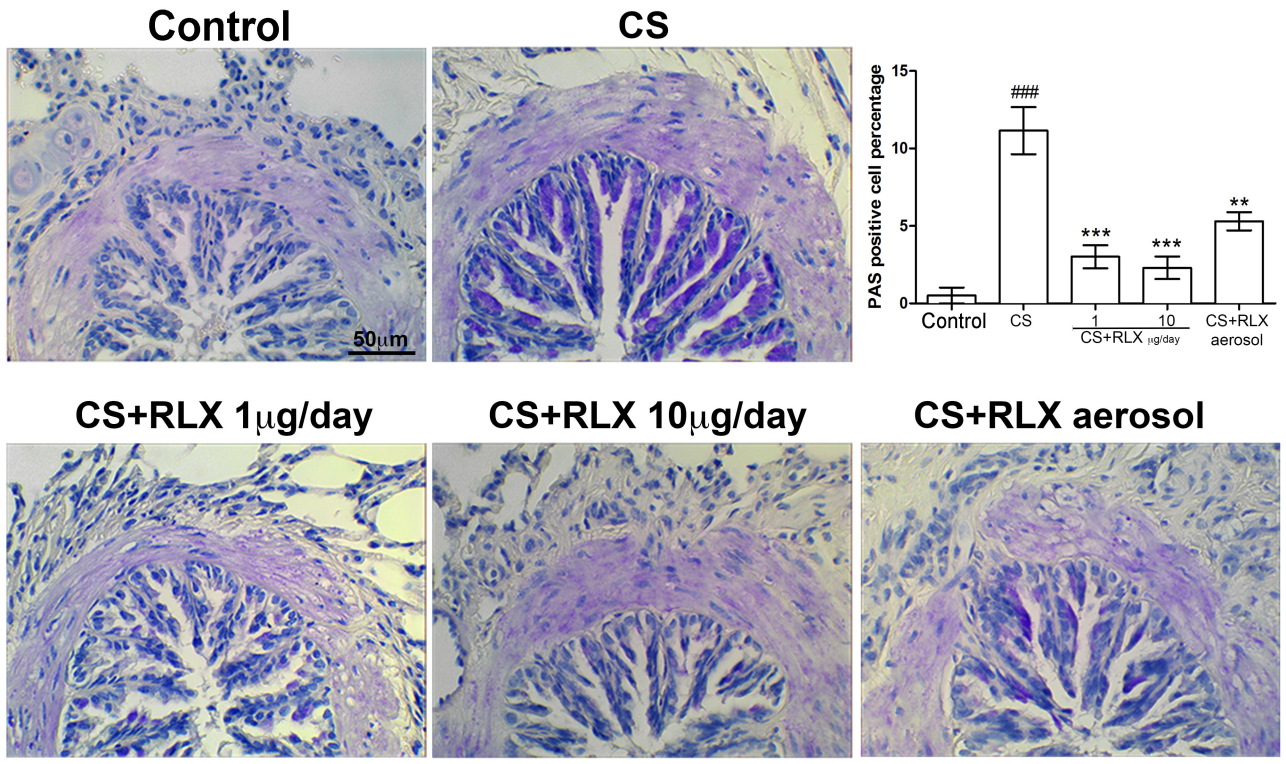
Control
CS
50μm
PAS positive cell percentage
15
10
5
0
###
***
***
**
Control
CS
1
10
CS+RLX μg/day
CS+RLX aerosol
CS+RLX 1μg/day
CS+RLX 10μg/day
CS+RLX aerosol

Figure 5

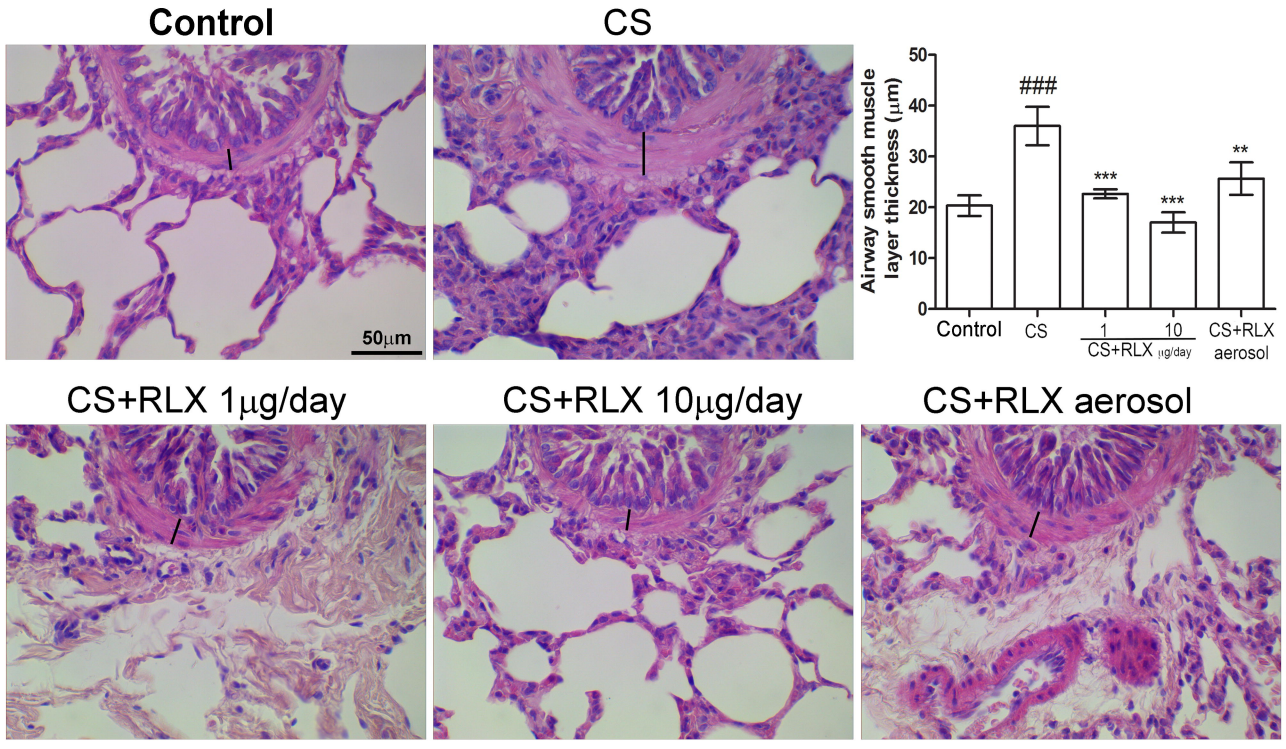
Control
CS
50μm
Airway smooth muscle layer thickness (μm)
50
40
30
20
10
0
###
***
***
**
Control
CS
1
10
CS+RLX μg/day
CS+RLX aerosol
CS+RLX 1μg/day
CS+RLX 10μg/day
CS+RLX aerosol

Figure 6

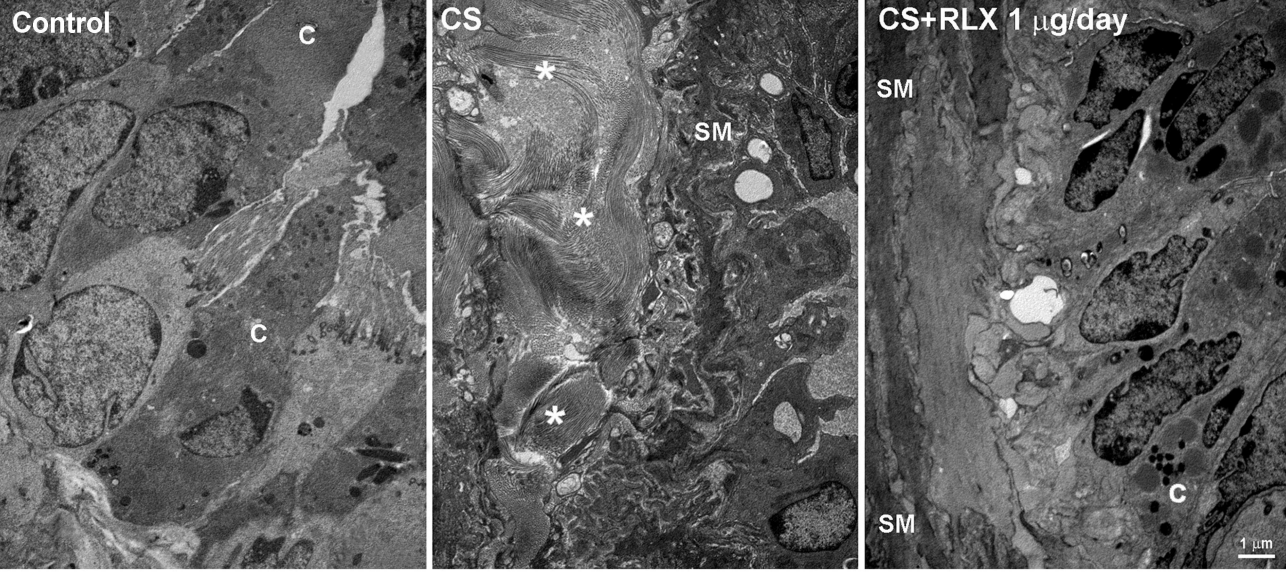

Figure 7